

Behavior of Stiffened Cold-Formed Steel Channel Sections Under Axial Compressive Force

Amr B. Saddek^{1,2}, Asmaa Y. Hamed³, Ahmed S. Tohamy^{4,*}

¹ Civil Engineering Dep., Faculty of Engineering, Al-Baha University, Al-Baha, Saudi Arabia

² Civil Engineering Dep., Faculty of Engineering, Beni-Suef University, Egypt

³ Construction and Building Dep., The Higher Institute of Engineering and Technology, Luxor, Egypt

⁴ Construction and Building Dep., The Higher Institute of Engineering and Technology, Minia, Egypt

* Corresponding author(s) E-mail: sedky_t2000@yahoo.com

ARTICLE INFO

Article history:

Received: 12 October 2024

Accepted: 16 January 2025

Online: 2 March 2025

Keywords:

Cold-formed steel,
Axial Compressive Force,
Deflection,
Local failure,
overall failure,
Initial imperfection

ABSTRACT

Cold-formed steel members (CFS) are gaining popularity and increasing importance due to their construction from thin sheet steel, making them more susceptible to local buckling. This study conducts a theoretical analysis focused on the examination of stiffened cold-formed members under axial compressive force. The factors influencing the behavior of compressed stiffened cold-formed members are identified through collapse load curves. A case study is conducted using a channel section of the cold-formed section with and without web stiffener for varying lengths. The theoretical analysis is applied to a pin-ended strut consisting of the two flanges without modification for the effective width of the web. The results are then compared with the recommendations of BS5400 based on the Perry-Robertson formula for estimating the collapse stresses formula. The findings indicate that the mathematical modeling in this study can elucidate the interactive buckling behavior of stiffened cold-formed members and provide valuable insights into the effect of web stiffener of channel section when used as cold-formed members, with the web stiffener consistently altering the mode of failure from local failure or interactive failure to overall failure.

1. Introduction

Cold-formed steel members (CFS) in structures are a significant advancement in the evolution of steel structures, with these members becoming increasingly popular as primary load-carrying elements in buildings. To enhance buckling resistance, more intricate shapes are being designed, as illustrated in Figure 1. Extensive research, both experimental and numerical, on the behavior of CFS sections has demonstrated that incorporating intermediate web stiffeners and edge stiffeners can significantly improve the strength of these sections. The thinness of the material allows for a more efficient use of resources, but it also poses challenges in terms of design limitations, such as restricted compression capacities due to low flexural and torsional stiffness [1]. These elements, due to their high slenderness ratio, are susceptible to two types of buckling: local buckling within the cross-section elements, which are typically divided into web plate and flange plate elements, and overall buckling along the member's length. Ye and Becque [2] conducted a study on cold-formed steel (CFS) plain and lipped channels subjected to axial compression, focusing on the interaction between local and overall flexural buckling. The results of this study were utilized to validate the accuracy of design procedures outlined in Eurocode 3 and to assess a proposed optimization technique. In a separate study, Young and

Rasmussen [3,4,5] investigated the ultimate capacity of CFS columns in channel form (plain and lipped) under pinned and fixed-ended boundary conditions. Their results indicated a noticeable shift in the effective centroid due to local buckling in pinned columns, while this effect was absent in fixed-ended columns. Furthermore, Loughlan and Yidris [6] explored the impact of local support conditions on the local-flexural interactive behavior of fixed-ended plain channels using numerical analysis.

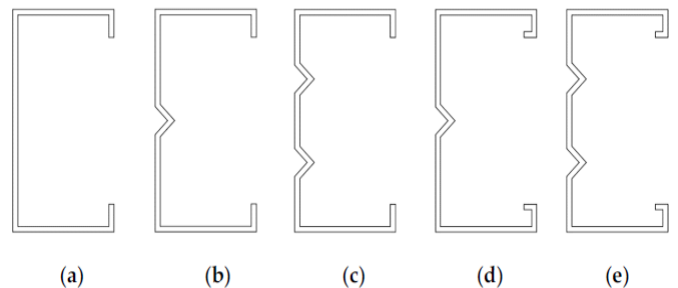


Figure 1: Different cross-sections of (a) A simple lipped channel; (b) A lipped channel with one web stiffener; (c) A lipped channel with two web stiffeners; (d) A channel section with one web stiffener and return lips; (e) A channel section with two web stiffeners and return lips

The study concluded that the support conditions at the plate ends significantly influence the behavior of the column, particularly under loads exceeding the local buckling threshold. Batista [7] applies the effective section method, ESM, as a continuation of the original effective area method, EAM. ESM has been effectively utilized in diverse engineering scenarios. In CFS Design, ESM is employed to accommodate local buckling effects. By taking into account the actual local buckling outcomes of the section, ESM offers more precise forecasts of member behavior and resistance, aiding in the optimization of cross-sectional dimensions and evaluation of stability under different loading conditions.

Manikandan et al. [8] conducted a numerical and experimental investigation into the behavior of cold-formed steel (CFS) channel sections with intermediate web stiffeners and outward lips under axial compression. The addition of a simple spacer plate externally to the channel section in the transverse direction was found to enhance the distortional buckling strength of the selected section. The finite element software ANSYS was utilized for the numerical analysis, which was then validated using experimental results. The study concluded that the presence of spacer plates can increase the axial capacity of stiffened CFS channel sections by 32%. Additionally, Fang et al. [9,10] examined local, distortional, and interactive modes of buckling for CFS sections under different loading conditions. Beulah [11] investigated the behavior of both lipped and unlipped channel sections with different slenderness ratios when subjected to axial force. This study involved a comparison with various international codes of practice, including the Indian Standard Code of Practice for the use of Cold-formed Light Steel Structural Members-IS:801, the British Code of Practice for Design of Cold-formed Sections-BS:5950 (Part 5), and the North American Standard- NAS Manual. Numerical analysis was carried out on the post-buckling behavior of channels under axial compression and compared with the specifications of previous codes. The study compared the load-carrying capacities versus axial shortening of lipped and unlipped channels with different slenderness ratios. It was observed that, in the case of an unstiffened element, the slenderness ratio of 30 to 100 combined local buckling, flexural buckling occurs about the minor axis, and for sections having a slenderness ratio of 120 to 200 overall flexural buckling occurs about the weak axis. Hajirasouliha et al. [12] introduced an optimized method for designing laterally braced and unbraced columns using lipped channel sections under axial loading conditions. They noted a significant 75% enhancement in lateral strength. In a separate study, Dinis and Camotim [13] delved into the behavior of columns with hat, zed, and rack-shaped sections in relation to local distortional buckling. The research also discussed the local-distortional interaction that impacts the failure mode and load-carrying capacity. Furthermore, Hajirasouliha and Becque [14] suggested the appropriate selection of lipped channel sections by analyzing the interaction between local and overall flexural buckling modes. Aswathy and Kumar [15] demonstrated that reducing the stiffness or depth of the lip in stiffened and unstiffened lipped channel sections during axial loading can lead to an increased risk of distortional buckling. Additionally, Kumar and Kalyanaraman [16] highlighted that the strength of compression members composed of CFS lipped channel sections diminishes due to the interaction between buckling modes during

axial loading. They emphasized the necessity of employing the direct strength method approach to accurately predict load and buckling interaction for individual buckling modes. Finally, Dar et al. [17] opted to study short columns experimentally instead of slender columns based on numerical investigations. Their findings indicated that the ultimate capacity of the column is influenced by the slenderness ratio, which impacts the behavior of battens in the built-up column under loading conditions.

2. Research significance

The (CFS) subjected to axial loading may experience buckling through one of three modes: local, overall, or interactive buckling, which is a combination of the first two modes. Local buckling can occur within the cross-section component, while overall buckling can occur in the overall direction of the member. The potential failure modes can be categorized as follows:

- 1- Overall failure if overall buckling occurs before local buckling.
- 2- Local failure if local buckling occurs before overall buckling.
- 3- Interactive failure if both overall and local buckling happen simultaneously.

The current investigation aimed to analyze the interactive buckling behavior of axially loaded channels, a topic that has been explored by various researchers. Abdel-Lateef [18,19] introduced an analytical method to study the non-linear interactive buckling behavior of such structural members until reaching the ultimate load, considering both local and overall initial imperfections. Gamal-Eldin [20] utilized the finite element method to analyze the interaction behavior of initially deflected and eccentrically loaded thin-walled channel sections, with the calculated critical stress incorporating local buckling effects. Ohaga et al. [21] employed the transfer matrix method to address elastic buckling issues of cold-formed steel (CFS) members with constant and variable thickness cross-sections. Khong [22] proposed a semi-numerical technique to reduce matrix size in the conventional finite element method, specifically applicable to thin-walled structures with sudden changes in thickness or material properties in the transverse direction. Kiong [23] introduced a finite element approach that combines the one-dimensional beam-column and modified thin plate element, representing the flange as a beam-column element and the web as a single plate element.

3. Analysis

CFS can experience failure in compression due to local, distortional, or overall buckling, as well as any potential interaction between these modes. Depending on factors such as the slenderness ratio of cross-section elements, loading conditions, and end boundary conditions, one of the buckling modes or a combination of buckling modes may manifest [24-27]. In this study, the approach involved separately estimating overall buckling and local buckling, with and without web stiffeners, and then analyzing the impact of these elements on the interactions of buckling modes. The influence of axial load on CFS resulted in the following sequence of events, illustrated in Figure 2:

- a) The bending stress distributions applied to a locally buckled member.

- b) An increase in compressive stress on the concave side, leading to a further reduction in effective width.
- c) Unloading occurring on the convex side of the member, causing parts of the elastically buckled plate to become effective again, resulting in a shift of the web-centered axis to a new position [26].

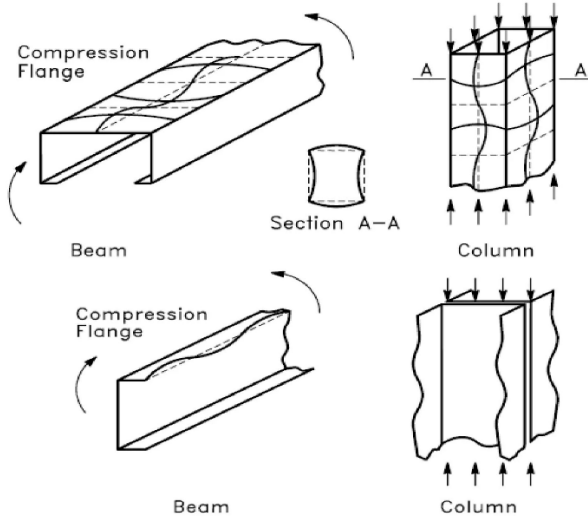


Figure 2: Effect of axial load on CFS with different sections

The displacement of the neutral axis can be illustrated as a compressive force (CFS) that is applied eccentrically at a distance (e), considering initial imperfections as a secondary influence on these structural elements, as depicted in Figure 3.

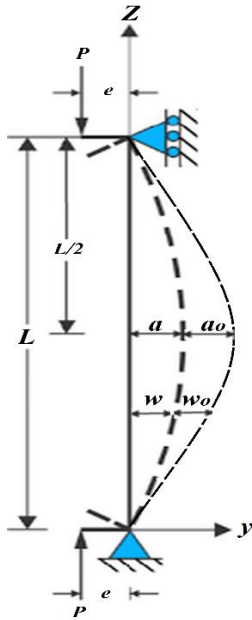


Figure 3: Effect of initial imperfection on overall buckling for eccentrically loaded member

3.1. Generating the Post-Buckling Equations

The deflection shape w of the buckled plate is determined by the physical boundary conditions. The buckled shape of simply supported rectangular plate (a, b) as shown in Figure 4 are described by Fourier series as follows,

$$z = \sum_{m=1}^{\infty} \sum_{n=1}^{\infty} A_{mn} \sin \frac{n\pi}{a} x \sin \frac{m\pi}{b} y \quad (1)$$

The half-wave length a depends on the plate (web) edges restraint, i.e., on the torsional stiffness of the cross-section flanges. The value of ($a = b$) corresponds to simply supported web edges (flanges with negligible torsional rigidity). At critical load the flat state of the plate becomes unstable, and new stable forms with deflection takes place, whose shape determined from the following differential equations,

$$\frac{\partial^4 z}{\partial x^4} + 2 \frac{\partial^4 z}{\partial x^2 \partial y^2} + \frac{\partial^4 z}{\partial y^4} = \frac{t}{D} \left[\sigma_x \frac{\partial^2 z}{\partial x^2} + \sigma_y \frac{\partial^2 z}{\partial y^2} - 2\tau_{xy} \frac{\partial^2 z}{\partial x \partial y} \right] \quad (2)$$

When using airy stress function ϕ , Eq. (2) may be written as follows,

$$\frac{\partial^4 \phi}{\partial x^4} + 2 \frac{\partial^4 \phi}{\partial x^2 \partial y^2} + \frac{\partial^4 \phi}{\partial y^4} = \frac{t}{D} \left[\ddot{\phi} \frac{\partial^2 z}{\partial x^2} + \phi'' \frac{\partial^2 z}{\partial y^2} - 2\dot{\phi} \frac{\partial^2 z}{\partial x \partial y} \right] \quad (3)$$

Where; $\sigma_x = \ddot{\phi}$, $\sigma_y = \phi''$, and $\tau_{xy} = -\dot{\phi}$

The compatibility equation of flat plate since follows,

$$\phi'''' + 2\phi'' \ddot{\phi} + \ddot{\phi} \phi'' = E[z'^2 - z''\dot{z}] \quad (4)$$

Assume that the buckled web plate waving and the physical boundary conditions as square plate as shown in Figure (4).

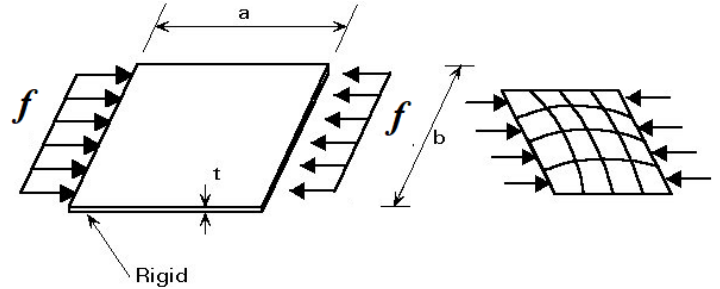


Figure 4: Deflection shape for plate buckling

The deflection shape z shown determined as follows:

$$z = A_1 \cos \frac{\pi}{a} x \cos \frac{\pi}{a} y + A_2 \sin 2 \frac{\pi}{a} x \sin 2 \frac{\pi}{a} y \quad (5)$$

If the plate being initially imperfect then the imperfection functions being as follows,

$$z_o = A_o \cos \frac{\pi}{a} x \cos \frac{\pi}{a} y \quad (6)$$

The solutions of Eqs. (3), and (4) has been derived for combined loading by [26]. Herein, the solution is being dominated for case of compression only as follows,

1. Assume that the stress function may be written as,

$$\phi = \phi_1 + \phi_2 \quad (7)$$

where; ϕ_1 , and ϕ_2 are a particular solution and a complementary solution for the biharmonic equation,

$$\phi'''' + 2\phi'' + \phi = 0 \quad (8)$$

Substituting the deflection function in Eq. (6) and replaces w by $(z - z_0)$,

Boundary conditions without taking the effect of shear stresses term are,

$$\text{At } x = \pm \frac{a}{2} \quad , \text{ and at } y = \pm \frac{a}{2}$$

$$\left(\frac{1}{a} \int_{-\frac{a}{2}}^{\frac{a}{2}} \phi \, dy = \sigma_x \right) \quad , \text{ and } \left(\frac{1}{a} \int_{-\frac{a}{2}}^{\frac{a}{2}} \phi'' \, dx = 0 \right)$$

The general solution of stress function ϕ in Eq. (7) for compression case only was found to be,

$$\begin{aligned} \phi = & -A_1^2 \frac{E}{32} (\cos 2\beta x + \cos 2\beta y) + \\ & A_2^2 \frac{E}{32} (\cos 4\beta x + \cos 4\beta y) - \\ & A_1 A_2 \frac{E}{25} (\sin \beta x \sin 3\beta y + \sin 3\beta x \sin \beta y) - \frac{\sigma_{xa}}{2} y^2 + \\ & A_0^2 \frac{E}{32} (\cos 2\beta x + \cos 2\beta y) \end{aligned} \quad (9)$$

where; σ_{xa} : is the applied stresses, $\beta = \frac{\pi}{a}$.

The form of Eq. (9) satisfies the boundary conditions without placing conditions on the unknown coefficients A_1, A_2 .

Applying Galerkin's method for the Eq. (3) for determine the unknown terms A_1, A_2 as follows,

$$\int_{-\frac{a}{2}}^{\frac{a}{2}} \int_{-\frac{a}{2}}^{\frac{a}{2}} \left[D \left(z'''' + 2z'' + z - t(z''\phi - 2z'\phi' + z\phi'') \right) \right] \times A_1 \cos \beta x \cos \beta y \, dx \, dy = 0 \quad (10)$$

$$\int_{-\frac{a}{2}}^{\frac{a}{2}} \int_{-\frac{a}{2}}^{\frac{a}{2}} \left[D \left(z'''' + 2z'' + z - t(z''\phi - 2z'\phi' + z\phi'') \right) \right] \times A_2 \sin 2\beta x \sin 2\beta y \, dx \, dy = 0 \quad (11)$$

After applying Galerkin's method in Eq. (10 and 11) based on the integral factors have been computed by Abdel-Lateff [18-19] the follows equations are obtained,

$$(A_1 - A_0) - 0.34A_1A_0^2 - A_1C + 0.88A_1A_2^2 = 0 \quad (12)$$

$$16A_2 - 4A_2C + 5.5A_2^3 + 0.88A_1A_2^2 = 0 \quad (13)$$

The stresses of web plate corners σ_x, σ_y shown in Figure (6), may written as follows,

$$\frac{\sigma_x}{\sigma_{cr}} = -0.34 (A_1^2 + 4A_2^2 + 3.2A_1A_2) - C = 0 \quad (14)$$

$$\frac{\sigma_y}{\sigma_{cr}} = -0.34 (A_1^2 + 4A_2^2 + 3.2A_1A_2) = 0 \quad (15)$$

Where: C is the ratio between the applied normal stress to the critical stress of the web plate.

The member can fail under a greater force and deflection if the web plate is provided with web stiffener as shown in Figure (5),

If the deflection function w and the initial imperfection w_0 written as follows,

$$w = a \sin \frac{m\pi}{L} x, \quad w_0 = a_0 \sin \frac{m\pi}{L} x \quad (16)$$

The ultimate force after applying principle of Energy method [26],

$$P = \frac{P_{cr}a}{a+a_0+1.27e} \quad (17)$$

From bending theory, the normal stress (stress in overall direction) equal to,

$$f_{xa} = - \left(\frac{P}{A} + w P_{cr} \frac{h}{I_y} \right) \quad (18)$$

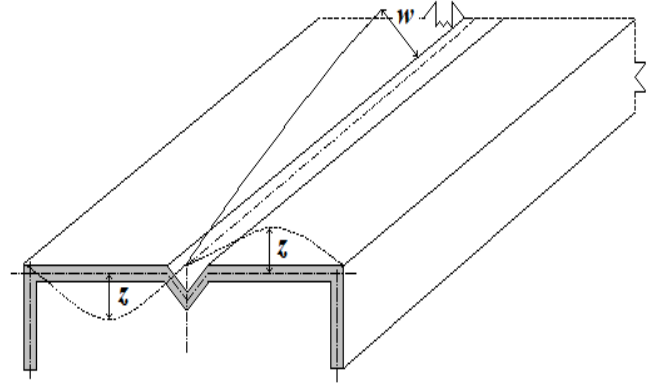


Figure 5: Effect of web stiffener on local buckling of web where the critical stress at this case is,

$$f_{cr} = \frac{16\pi^2 E}{12(1-\nu^2)} \left(\frac{t}{b} \right)^2 \quad (19)$$

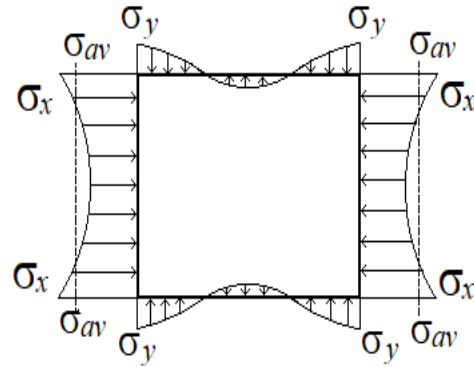


Figure 6: Stresses Distribution at the Plate Corners

The equivalent stress is computed according to Von-miss equation as follows,

$$\sigma_{eq} = (\sigma_x^2 + \sigma_y^2 - \sigma_x \sigma_y)^{0.5} \quad (20)$$

When considering the relationship between the applied stress and the average strain over the length of the plate, there are two stiffness factors n_t, n_s as follows:

The elastic tangent stiffness of the plate n_t represents the local slope of the curve related to the average applied stress and the average strain or the local elastic stiffness of the plate.

The secant stiffness n_s is defined as the ratio between the applied stresses and the corresponding strain at each load level.

Initially, the web exhibits a local imperfection z_0 , which leads to a reduced stiffness and thus to an effective second moment of area of the entire cross-section even before the load is applied.

$$b_e = n_t b \quad (21)$$

The stress at this case equal to,

$$\sigma_{xa} = -n_s \left(\frac{P}{A_r} + w P_{cr} \frac{h}{I_y} \right) \quad (22)$$

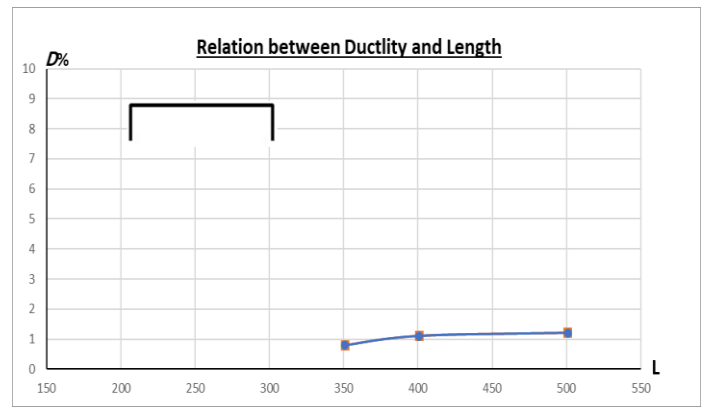
The reduced values of stress produce another value of C , then through previous equations, the applied stress on the member will reach its maximum, s_{max} , when s_{eq} reaches the material yield stress s_y .

4. RESULTS And Discussion

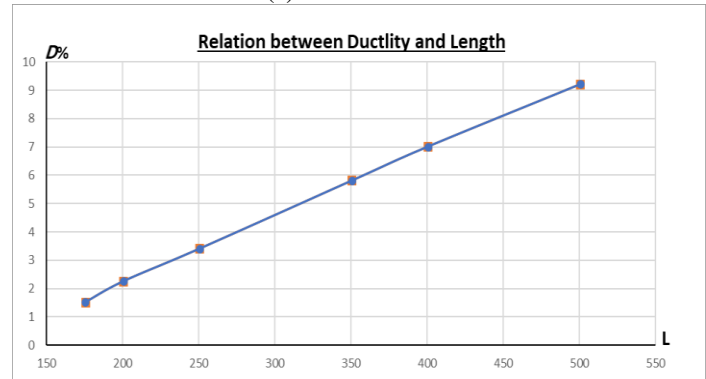
As already explained, the (CFS) can buckle in one of three modes under axial loading. These modes are local buckling, general buckling and interactive buckling as a combination of the first two modes. This paper shows how web stiffening helps to change the buckling modes from local or interactive buckling to general buckling modes. The economic use of (CFS) when collapse is due to general buckling would be similar to hot rolled sections that do not suffer from local buckling.

Fig.(7-a) and (7-b) show that, the ductility in the case of web stiffening changes linearly with the length of the component and can be predicted for different lengths. On the other hand, the same relationships are not linear if the web is not stiffened in the cross-section. Figs. (8-a) and (8-b) show that for different degrees of initial imperfection, the initial slopes of the curves of the relationships between the bearing capacity and the deflection are higher in the case of the web cross-section with stiffening than in the case of the web cross-section without stiffening. Fig. (9-a) and (9-b) show that the effect of the web stiffener on the increase of the bearing capacity at different degrees of initial imperfection, the curves of the relationships between length and bearing capacity also increase steadily in contrast to the same web cross-section without stiffener.

As this research is discussing the behavior of stiffened (CFS) under compression through a theoretical analysis based on some assumptions. Therefore, the results of computer program should be compared with the recommendation of the BS5400 [28], based on Perry-Robertson formula for estimating the collapse stresses, where this formula is treated for pin ended strut consisting of the two flanges and without modification for the effective width of the web. These curves were drawn together with the curves from the present analysis. For high accuracy this formula is used in this research for check the results in cases of overall initial imperfection only, as this formula is used for hot rolled sections which are not suffer from local buckling. Figs.(10-a) and (10-b) show the comparison of results when applying of the Perry-Robertson formula on the basic cross sections provided with or without web stiffener for length ($L= 4000\text{mm}$).

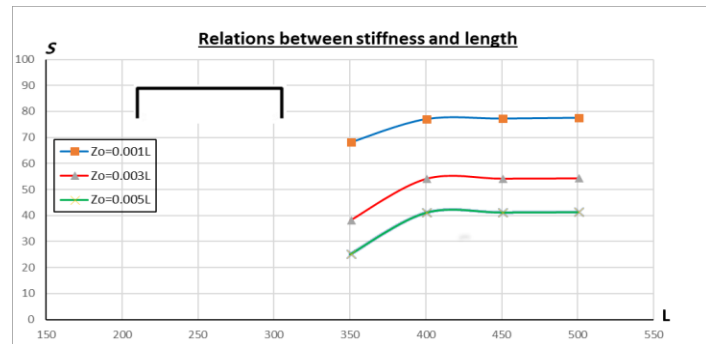


(a) Normal section

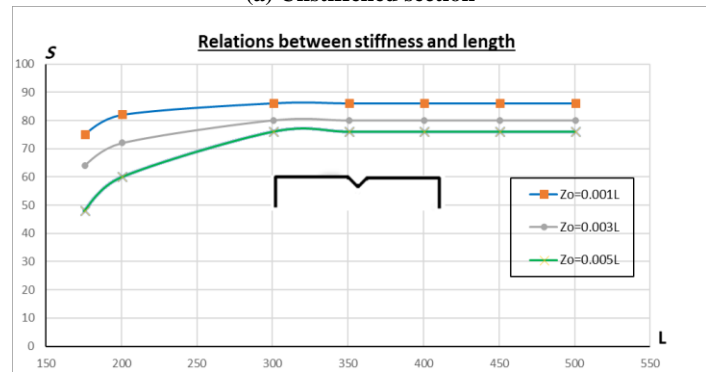


(b) Stiffened section

Figure 7: Ductility percentage for normal section and stiffened section

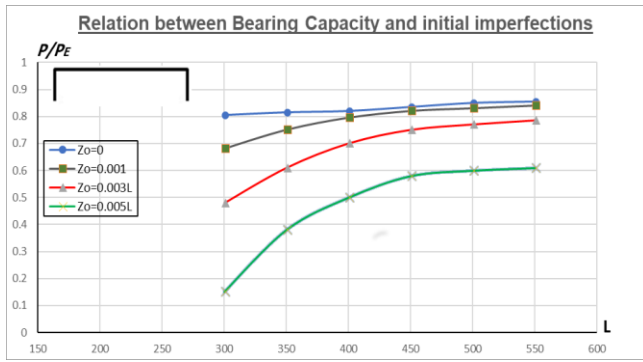


(a) Unstiffened section

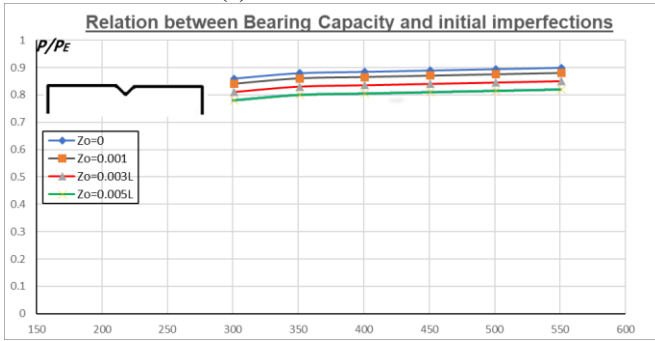


(b) Stiffened section

Figure 8: Relations between stiffness and length for unstiffened and stiffened section

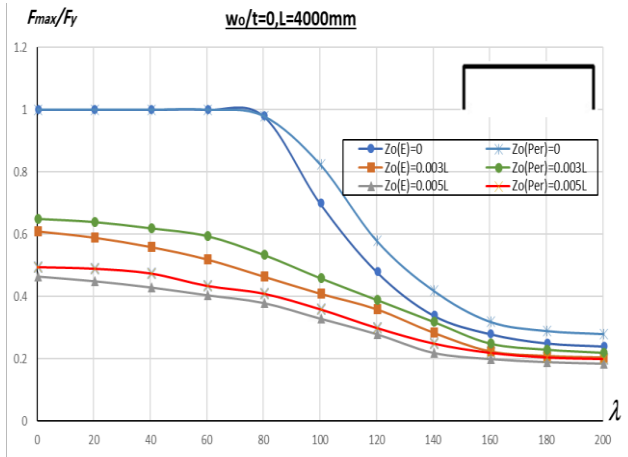


(a) Unstiffened section

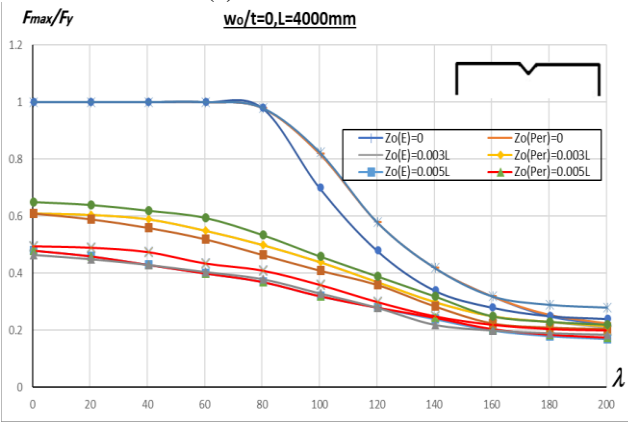


(b) Stiffened section

Figure 9: Relations between bearing capacity and length for unstiffened and stiffened section



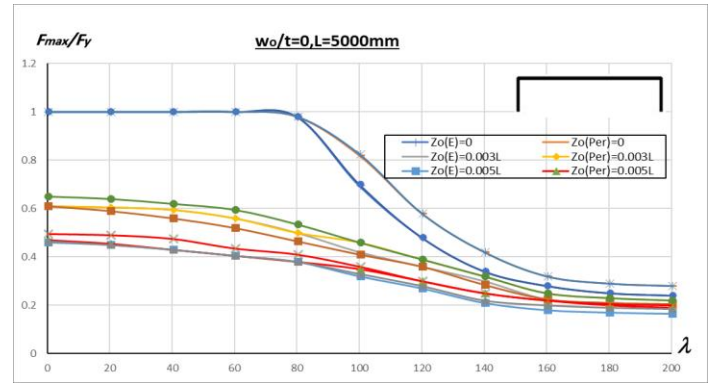
(a) Unstiffened section



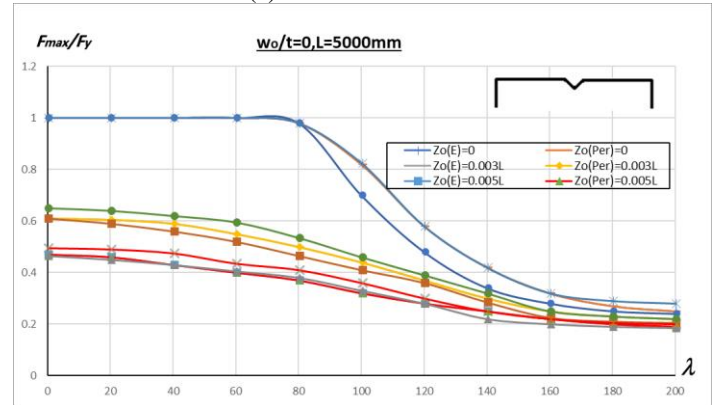
(b) Stiffened section

Figure 10: Collapse stresses for local failure for unstiffened and stiffened section

The effect of web stiffener is remarked in changing the mode failure of member from local failure to overall failure. The difference between results at this case is very clear because local failure is mainly based on that the member is collapse as a result local buckling, but Perry-Robertson formula depends mainly on overall buckling. Figs.(11-a) and (11-b) for (CFS) with length ($L=5000$ mm) show the effect of web stiffener in changing the mode failure of member from interactive failure to overall failure, but for this case the difference between results is more nearly than previous case. Figs.(12-a), and (12-b) show (CFS) with length ($L=6000$ mm), the comparison between results from Perry-Robertson formula, as in this case the effect of web stiffener on in changing results may be negligible.



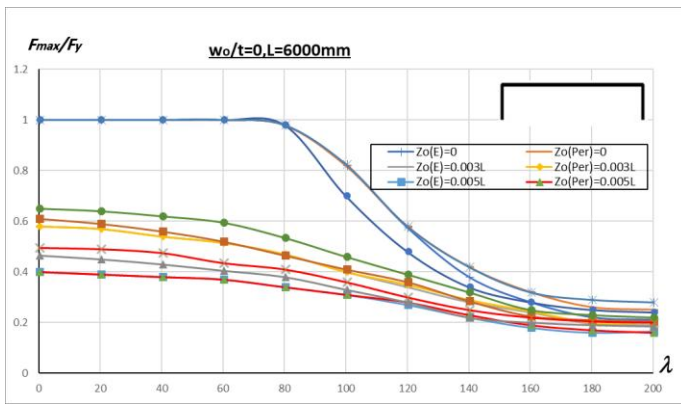
(a) unstiffened section



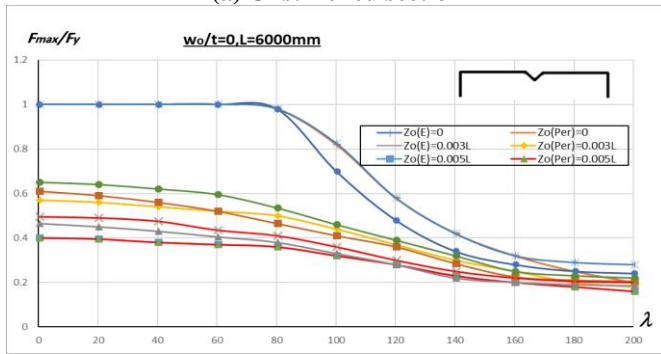
(b) Stiffened section

Figure 11: Collapse stresses for overall failure

It can be seen from these figures, that if the (CFS) being with high slenderness ratio, then the member fails by the overall failure where the results are nearly approximately at different degree of slenderness ratio, and for different degree of overall initial imperfections. These remarks are due to disappear effect of local buckling and the collapse is being due to overall buckling only. Also, it is very important to notice, that the present work is considering the movement of the neutral axis position due to plate buckling. Due to this effective, a change in neutral axis position is takes place and the applied concentric load induced bending.



(a) Unstiffened section



(a) Stiffened section

Figure 12: Collapse stresses for overall failure

5. Conclusions

The mathematical modeling for the interactive buckling explained in this paper can make a useful contribution by providing a mean of explaining the behaviour of stiffened (CFS). So far, we have considered the effect of web stiffener in reducing the local buckling effect for both of perfect and imperfect members.

This paper shows the effect of web stiffener on the behaviour of compression (TWM) through the following results,

1. The web stiffener always change mode of failure from local failure or interactive failure to overall failure.
2. Overall failure for compression (CFS) is approximately as the failure of hot-rolled sections.
3. The stiffener for compression (CFS) fails by overall failure may be negligible.
4. The relations between ductility and length at case of web stiffener is at linear form.
5. The relations between ductility and length at case of normal section is at non-linear form.
6. Web stiffeners rise the stiffness of the thin-walled compression member.

Conflict of Interest

The authors declare no conflict of interest.

Symbols

CFS	Cold Formed Steel.
L, b, t	Length of member, width and plate thickness.
I	Moment of inertia of cross section.
A	Area of cross section.
P	Applied compression force.
P_E	Euler's critical load $=\pi^2 EI/L^2$
f_{xa}	Stress in overall direction.
$F_{y,E}$	Material yield stress and Modulus of Elasticity.

References

- [1] S. T. Vy, M. Mahendran, "Behaviour and design of slender built-up nested cold-formed steel compression members", Engineering Structures, Volume 241, 15 August 2021, 112446.
- [2] J. Y., I. Hajirasouliha, J. Becque, "Experimental investigation of local-flexural interactive buckling of cold-formed steel channel columns", Thin-Walled Struct., 125 (2018), pp. 245-258.
- [3] B. Young, K.J.R. Rasmussen, "Tests of fixed-ended plain channel columns", J. Struct.Eng., ASCE 124 (2) (1998) 131-139.
- [4] B. Young, K.J.R. Rasmussen, "Behaviour of cold-formed singly symmetric columns", Thin-Walled Struct. 33 (1999) 83-102.
- [5] B. Young, K.J.R. Rasmussen, "Shift of effective centroid of channel columns", J.Struct. Eng., ASCE 125 (2) (1999) 524-531.
- [6] J. Loughlan, N. Yidris, "The local-overall flexural interaction of fixed-ended plain channel columns and the influence on behaviour of local conditions at the constituent plate ends", Thin-Walled Struct. 81 (2014) 132-137.
- [7] E.M. Batista, "Effective section method: a general direct method for the design of steel cold-formed members under local-global buckling interaction", Thin-Walled Struct. 48 (2010) 345-356.
- [8] P. Manikandan, Balaji Shanmugam, and Krishanu Roy, "A Novel Approach to Improve the Distortional Buckling Strength of a Stiffened Cold-Formed Steel Channel Section under Axial Compression", Structural Design and Construction, 28 (1) (2023), Vol. 28, No. 1-8.
- [9] Z. Fang, K. Roy, B. Chen, C.W. Sham, I. Hajirasouliha, and J. B. P. Lim. a., "Deep learning-based procedure for structural design of cold formed steel channel sections with edge-stiffened and un-stiffened holes under axial compression.", Thin-Walled Struct. 166 (Sep) 2021.
- [10] Z. Fang, K. Roy, D. Lakshmanan, P. Pranomrum, F. Li, H. H. Lau, and J. B. P. Lim, "Structural behaviour of back-to-back cold-formed steel channel sections with web openings under axial compression at elevated temperatures.", J. Build. Eng. 54 (Aug): 2022 .
- [11] G. Beulah Gnana Ananthi, " Performance of Plain and Lipped Cold-Formed Channel Sections in Axial Compression", International Journal of Earth Sciences and Engineering, Volume 09, No. 04, August 2016, P.P.885-887.
- [12] Y, J. Hajirasouliha; I.J. Becque; A. Eslami, "Optimum design of cold-formed steel beams using Particle Swarm Optimization method.", J. Constr. Steel Res. 2016, 122, 80-93 .
- [13] P.B. Dinis, D. Camotim, "Cold-formed steel columns undergoing local-distortional coupling: Behaviour and direct strength prediction against interactive failure.", Comput. Struct. 2015, 147, 181-208.
- [14] Y, J. Hajirasouliha, I. Becque, J., "Experimental investigation of local-flexural interactive buckling of cold-formed steel channel columns.", Thin-Walled Struct. 2018, 125, 245-258.
- [15] K.C.K. Aswathy, M.V.A. Kumar, "Unstiffened Elements as Limiting Case of Distortional Buckling of Partially Stiffened Elements.", J. Struct. Eng. 2020, 146, 04020171.

- [16] M.V.A. Kumar; V. Kalyanaraman, "Interaction of Local, Distortional, and Global Buckling in CFS Lipped Channel Compression Members.", *J. Struct. Eng.* 2018, 144, 04017192 .
- [17] M.A. Dar.; D.R. Sahoo.; A.K. Jain, " Numerical Study on the Structural Integrity of Built-up Cold-Formed Steel Battened Columns"; Springer Nature: Singapore, 2020; pp. 815–823 .
- [18] T.H. Abdel-Lateef, "Buckling of Stiffened Plates subjected to combined Shear and Compression Loading", Ph. D. Thesis, University College London, November 1982.
- [19] T.H. Abdel-Lateef, "Interactive Buckling of Thin-Walled Columns", Third Arab Structural Conference, The United Arab Emirates University, Vol.1, pp.88-108, 5-8 March 1988.
- [20] A. Gamal-Eldin, "The effect of Local Instability on the Global Instability for Thin-Walled Channel Sections for Two Different Loading Conditions", First International Conference on Civil Engineering, Hellwan University, pp.598-635, 24-26 March 1998.
- [21] M. Ohga, T. Shigematsue, and K. Kawaguchi, "Buckling Analysis of Thin-Walled Members with Variable Thickness", *Journal of Structural Engineering*, Vol.121, No.6, June 1995.
- [22] P.W. Khong, , "The Comparison of Lower Order and Higher Order Finite Strip Analysis in the Stability Problem of Thin-Walled Structures", *Journal of Computer and Structures*, Vol.36, No.1, pp.109-118, 1990.
- [23] C.C. Kiong, , G.A. Faris, and S.F. Kitipornchai, "Finite Element Method for Buckling Analysis of Plate Structures", *Journal of Structural Engineering*, Vol.119, No.4, pp.1048-1067, April 1993.
- [24] P. Manikandan, T. Pradeep., "Effective Cross Section of Cold Formed Steel Column Under Axial Compression", *J. Inst. Eng. India Ser.*, 14 February 2018, <https://doi.org/10.1007/s40030-018-0276-9>.
- [25] A. Y. Hamed, "Elastic Shear Buckling of Tapered Steel Plate Girders with Opening In Web," *Journal of Engineering Sciences (JES)*, vol. 51, no. 3, pp. 148-172; <https://doi.org/10.21608/JESAUN.2023.177464.1184>, 2023.
- [26] A. B. Saddek "Buckling of Cold Formed Members ", International Conference, El Minia, Egypt 21-23 Mars 1999
- [27] A. Y. Hamed, M. F. Hassanein and M. A. Hasan, "Stress-strain modelling of circular concrete-filled FRP–steel composite tube columns under axial compression load," *Structures*, vol. 67, pp. 107040, <https://doi.org/10.1016/j.istruc.2024.107040>, 2024.
- [28] B.S 5400-5:2005. (2005). *Steel, Concrete and Composite Bridges. Part 5: Code of Practice for Design of Composite Bridges*. British Standards Institution: London, UK, 1-48.